

Filtered finite difference methods for nonlinear Schrödinger equations in semiclassical scaling

Yanyan Shi¹, Christian Lubich¹

Abstract This paper introduces filtered finite difference methods for numerically solving a dispersive evolution equation with solutions that are highly oscillatory in both space and time. We consider a semiclassically scaled nonlinear Schrödinger equation with highly oscillatory initial data in the form of a modulated plane wave. The proposed methods do not need to resolve high-frequency oscillations in both space and time by prohibitively fine grids as would be required by standard finite difference methods. The approach taken here modifies traditional finite difference methods by incorporating appropriate filters. Specifically, we propose the filtered leapfrog and filtered Crank–Nicolson methods, both of which achieve second-order accuracy with time steps and mesh sizes that are not restricted in magnitude by the small semiclassical parameter. Furthermore, the filtered Crank–Nicolson method conserves both the discrete mass and a discrete energy. Numerical experiments illustrate the theoretical results.

Keywords. finite difference method, filter, nonlinear Schrödinger equation, semiclassical, highly oscillatory, asymptotic-preserving, uniformly accurate

Mathematics Subject Classification (2020): 65M06, 65M12, 65M15

1 Introduction

As a basic model problem of a dispersive evolution equation with solutions that are highly oscillatory in both space and time, we consider the time-dependent weakly nonlinear Schrödinger equation in semiclassical scaling [5, 6],

$$i\varepsilon \partial_t u + \frac{\varepsilon^2}{2} \Delta u = \lambda \varepsilon |u|^2 u, \quad (1.1)$$

¹ Mathematisches Institut, Univ. Tübingen, D-72076 Tübingen, Germany.
E-mail: {Lubich, Shi}@na.uni-tuebingen.de

which is to be solved for the complex-valued function $u = u(t, x)$ under periodic boundary conditions with $x \in \mathbb{T}^d = (\mathbb{R}/2\pi\mathbb{Z})^d$ over a bounded time interval $0 < t \leq T$ and with highly oscillatory initial data at $t = 0$:

$$u(0, x) = e^{i\kappa \cdot x / \varepsilon} a_0(x). \quad (1.2)$$

Here, $0 < \varepsilon \ll 1$ represents the semiclassical small parameter, and λ is a fixed nonzero real number. In the initial condition, $\kappa \in \mathbb{R}^d \setminus \{0\}$ is a fixed wave vector, and $a_0 : \mathbb{T}^d \rightarrow \mathbb{C}$ is a given smooth profile function with derivatives bounded independently of ε . The final time T is chosen independently of ε . On this time scale, the nonlinearity has an $O(1)$ effect on the solution.

The initial function $u(0, \cdot)$ in (1.2) is required to be a 2π -periodic continuous function. This is satisfied if the small parameter ε is assumed to take only values for which $\kappa/\varepsilon \in \mathbb{Z}^d$ and a_0 is 2π -periodic. This assumption on ε is not a restriction, since it can always be achieved with an $O(\varepsilon)$ modification of κ and a corresponding smooth modification of a_0 .

It is readily checked that there are two conserved quantities for (1.1) in any dimension $d \geq 1$: the mass

$$\int_{\mathbb{T}^d} |u|^2 dx = \text{const.}$$

and the energy

$$\int_{\mathbb{T}^d} \left(\frac{\varepsilon^2}{2} |\nabla u|^2 + \frac{\lambda \varepsilon}{2} |u|^4 \right) dx = \text{const.}$$

It is known that the solution $u(t, x)$ is highly oscillatory in both time and space at a scale proportional to the small semiclassical parameter ε . This poses significant challenges in the development of efficient numerical methods and their error analysis.

Traditional finite difference methods like the leapfrog and Crank–Nicolson schemes have been studied for Schrödinger-type equations in the semiclassical scaling [21], where stringent constraints on the time step $\tau \ll \varepsilon$ and mesh size $h \ll \varepsilon$ are required to guarantee accurate approximations of observables. Time-splitting spectral discretizations [2, 3, 17, 19] ease these restrictions, allowing for $\tau = O(\varepsilon)$, $h = o(\varepsilon)$ while still providing accurate results. Asymptotic-preserving methods have been proposed in [1, 7, 4] by reformulating the Schrödinger equation using the WKB expansion [10, 5] or the Madelung transform [20].

It is commonly believed that finite difference methods applied directly to (1.1) require very restrictive meshing conditions and are thus not suitable for solving the semiclassical Schrödinger equation. In this work, we aim to demonstrate the effectiveness of finite difference methods when enhanced with appropriate filtering. Specifically, we present two finite difference methods, constructed by applying appropriate filters to the leapfrog and Crank–Nicolson methods. *These filtered schemes enable us to approximate the solution of (1.1)–(1.2) with second-order accuracy even when using comparatively large time steps τ and mesh sizes h that are not restricted by ε .* The proposed filtered

methods tend to the standard leapfrog and Crank–Nicolson schemes as the ratios of the time step and mesh size to the semiclassical parameter ε approach zero, which is, however, not the regime of principal interest in this paper. The methods are not only asymptotic-preserving as $\varepsilon \rightarrow 0$ but are also uniformly accurate (of order $1/2$) for $0 < \varepsilon \leq 1$. Moreover, the filtered Crank–Nicolson scheme turns out to preserve the discrete mass and a modified discrete energy exactly.

For various classes of highly oscillatory ordinary differential equations, filtered time-stepping methods have already been used successfully, e.g., in [9, 16, 12, 15, 11, 14, 13]. Modulated Fourier expansions [15] are a powerful tool for deriving and analyzing numerical methods for highly oscillatory problems. They represent both the exact and the numerical solution as sums of products of slowly varying modulation functions and highly oscillatory exponentials. Comparing the modulated Fourier expansions of the numerical and the exact solution then yields error bounds. We shall pursue a related approach also here, for the first time combined in both time and space, which becomes possible under a consistency relation between the time step and the spatial mesh size.

We will formulate the filtered finite difference methods and prove results for them only in the spatially one-dimensional case ($d = 1$). This apparent limitation is introduced only for ease of presentation. The methods and the theoretical results can be extended to higher dimensions without additional difficulties. The extension to the full space \mathbb{R}^d instead of the torus \mathbb{T}^d is straightforward for the formulation of the methods and can be done analogously in the theory. The condition $\kappa/\varepsilon \in \mathbb{Z}^d$ imposed for 2π -periodicity is then no longer needed.

In Section 2, we introduce the filtered finite difference methods and state the main results of this paper. We give the dominant term of the modulated Fourier expansion of the numerical solution and prove second-order error bounds over a fixed time interval (independent of ε), with step sizes τ and meshwidths h that can be arbitrarily large compared to ε . For $h \gg \varepsilon$, there is a mild stepsize restriction $\tau \leq ch$ for the filtered leapfrog method and no such restriction for the filtered Crank–Nicolson method. However, the step size τ and the mesh width h cannot be chosen independently but are related by a consistency condition.

The results of Section 2 are proved in Sections 3 and 4. In Section 3 we study the consistency error, i.e., the defect obtained on inserting a function with controlled small distance to the exact solution into the numerical scheme. Section 4 first presents the linear Fourier stability analysis and then gives a nonlinear stability analysis that bounds the error of the numerical solution in terms of the defect.

In Section 5, numerical experiments are conducted to illustrate the theoretical results. We also present numerical experiments on the long-time behaviour of mass and energy with the filtered finite difference discretizations, which go beyond the analysis in this paper.

2 Numerical methods and main results

For simplicity of presentation, we introduce our two filtered finite difference methods in the context of one spatial dimension, $0 \leq x \leq 2\pi$, with periodic boundary conditions. Let the time step be $\tau = T/N > 0$ and the mesh size $h = 2\pi/M > 0$, where N and M are positive integers. We denote by u_j^n the numerical approximation of $u(t_n, x_j)$, where $t_n = n\tau$ for $0 \leq n \leq N$, and $x_j = jh$ for $0 \leq j \leq M$. The numerical methods and the theoretical results for them can be extended to higher space dimensions without additional difficulty.

Filtered leapfrog algorithm. We first introduce an explicit algorithm, which has the symmetric two-step formulation

$$i\varepsilon \frac{u_j^{n+1} - u_j^{n-1}}{2\tau \operatorname{sinc}(\alpha)} + \frac{\varepsilon^2}{2} \frac{u_{j+1}^n - 2\phi(\beta)u_j^n + u_{j-1}^n}{h^2 \psi(\beta)} = \lambda\varepsilon \frac{|u_j^n|^2 u_j^n}{\operatorname{tanc}(\alpha)} \quad (2.1)$$

with $\operatorname{sinc}(z) = \sin(z)/z$ and $\operatorname{tanc}(z) = \tan(z)/z$, and where

$$\begin{aligned} \phi(z) &= \frac{3}{2} \operatorname{sinc}(z) - \frac{1}{2} \cos(z), & \psi(z) &= \frac{\phi(z) - \cos(z)}{z^2/2}, \\ \alpha &= \frac{1}{2} \kappa^2 \tau / \varepsilon, & \beta &= \kappa h / \varepsilon. \end{aligned}$$

Note that as $z \rightarrow 0$, we have $\operatorname{sinc}(z) = 1 + O(z^2)$ and $\operatorname{tanc}(z) = 1 + O(z^2)$, and $\phi(z) = 1 + O(z^4)$ and $\psi(z) = 1 + O(z^2)$, so that the filtered leapfrog scheme tends to the classical leapfrog scheme in the limit $\tau/\varepsilon \rightarrow 0$ and $h/\varepsilon \rightarrow 0$. Our interest here is, however, to use the filtered scheme with large ratios τ/ε and h/ε .

Filtered Crank–Nicolson algorithm. We further present the following implicit scheme:

$$i\varepsilon \frac{u_j^{n+1} - u_j^{n-1}}{2\tau \operatorname{sinc}(\alpha)} + \frac{\varepsilon^2}{2} \frac{\tilde{u}_{j+1}^n - 2\phi(\beta)\tilde{u}_j^n + \tilde{u}_{j-1}^n}{h^2 \psi(\beta)} = \lambda\varepsilon \frac{(|u_j^{n-1}|^2 + |u_j^{n+1}|^2)\tilde{u}_j^n}{2 \operatorname{tanc}(\alpha)}, \quad (2.2)$$

with $\tilde{u}_j^n = (u_j^{n+1} + u_j^{n-1})/(2 \cos(\alpha))$. Scheme (2.2) gives the map $u^{n-1} \mapsto u^{n+1}$; using half the time step $\tau \rightarrow \tau/2$, it can be written and implemented as a one-step method $u^n \mapsto u^{n+1}$.

Note that as $\tau/\varepsilon \rightarrow 0$ and $h/\varepsilon \rightarrow 0$, this scheme tends to the classical Crank–Nicolson scheme. We are, however, interested in using the filtered scheme with large ratios τ/ε and h/ε .

Proposition 2.1 *The filtered Crank–Nicolson algorithm (2.2) conserves the following discrete mass and energy:*

$$\begin{aligned} \sum_j |u_j^n|^2 &= \text{const}, \\ \frac{\varepsilon^2}{2} \sum_j \frac{|u_{j+1}^n - u_j^n|^2}{h^2 \psi(\beta)} + \frac{\lambda\varepsilon}{2} \sum_j \frac{|u_j^n|^4}{\operatorname{tanc}(\alpha)} &= \text{const}. \end{aligned} \quad (2.3)$$

Proof These two conservation properties can be proved analogously to [8]. \square

The following result (Theorem 2.1) gives the dominant term of the modulated Fourier expansion of the numerical solutions of (2.1) and (2.2). Under appropriate assumptions, this term is the same term $a(t, x) e^{i(\kappa x - \kappa^2 t/2)}$ as for the exact solution of (1.1) (see [6]), where $a(t, x)$ solves the hyperbolic initial value problem

$$\partial_t a + \kappa \partial_x a = -i\lambda |a|^2 a, \quad a(0, x) = a_0(x). \quad (2.4)$$

To obtain the same dominant term for the numerical method, we need a relation between ε , τ and h . The step size and the mesh width are chosen such that $\alpha = \frac{1}{2}\tau^2/\varepsilon$ and $\beta = \kappa h/\varepsilon$ satisfy the following *consistency condition*: For a fixed nonzero real number ρ ,

$$\frac{\varepsilon}{\text{tanc}(\alpha)} = \frac{\varepsilon \text{sinc}(\beta)}{\psi(\beta)} = \rho. \quad (2.5)$$

Condition (2.5) ensures that the profile $a(t, x)$ satisfies the same equation (2.4) as for the exact solution.

For the filtered leapfrog method (though not for the filtered Crank-Nicolson method) we further need the following *stability condition*: for a fixed $\theta < 1$,

$$\frac{\varepsilon \tau}{h^2} |\text{sinc}(\alpha)| \frac{1 + |\phi(\beta)|}{|\psi(\beta)|} \leq \theta < 1. \quad (2.6)$$

When $h \gg \varepsilon$ with $\sin(\beta)$ bounded away from 0, the last factor on the left-hand side is proportional to h/ε^2 by (2.5). The second factor is $O(\varepsilon)$ by (2.5). Hence, condition (2.6) then reduces to requiring that τ/h be bounded by a sufficiently small constant independent of ε . Note that in contrast the standard leapfrog method has a time step restriction $\varepsilon \tau \leq h^2$ together with $\tau \ll \varepsilon$ and $h \ll \varepsilon$.

Theorem 2.1 (Dominant term of the numerical solution) *Let u_j^n be the numerical solution obtained by applying the filtered leapfrog algorithm (2.1) under the stability condition (2.6) or by the filtered Crank-Nicolson method (2.2) without requiring a stability condition, and in both cases under the consistency condition (2.5). Assume $a_0 \in C^4(\mathbb{T})$. Then, the numerical solution u_j^n can be written as*

$$u_j^n = a(t, x) e^{i(\kappa x - \kappa^2 t/2)/\varepsilon} + R(t, x)$$

for $t = n\tau \leq T$, $x = jh$, where $a(t, x)$ is the solution of (2.4) and the remainder term is bounded in the maximum norm by

$$\|R\|_{C([0, T] \times \mathbb{T})} \leq C(\tau^2 + h^2 + \varepsilon).$$

Here, C is independent of ε, τ, h , but depends on ρ and θ and the final time T .

A further main result of this paper is the following error bound for the two filtered finite difference methods, which follows directly from the representations of the numerical and exact solutions in Theorem 2.1 and in [6, Theorem 6.5], respectively.

Theorem 2.2 (Error bound) *Under the assumptions of Theorem 2.1, we obtain*

$$|u(t_n, x_j) - u_j^n| = O(\tau^2 + h^2 + \varepsilon)$$

uniformly for $t_n = n\tau \leq T$ and $x_j = jh$ both for the filtered leapfrog scheme and the filtered Crank–Nicolson method. The constant symbolized by the O -notation is independent of ε , time step τ and mesh size h subject to the consistency condition (2.5) and the stability condition (2.6) (the latter not needed for the filtered Crank–Nicolson method), and independent of j and n with $t_n \leq T$.

Remark 2.1 In the less interesting regime where $\tau \ll \varepsilon$ and $h \ll \varepsilon$, standard error analysis based on the Taylor series of the solution yields an $O((\tau^2 + h^2)/\varepsilon^3)$ error bound, so that the error is bounded by

$$|u(t_n, x_j) - u_j^n| \leq \min(C_0(\tau^2 + h^2 + \varepsilon), C_1(\tau^2 + h^2)/\varepsilon^3)$$

uniformly for $t_n = n\tau \leq T$, $x_j = jh$, and $0 < \varepsilon \leq 1$. The maximum of this error bound over $0 < \varepsilon \leq 1$ is attained for $\varepsilon^4 \sim \tau^2 + h^2$, which yields an $O((\tau^2 + h^2)^{1/4})$ uniform accuracy for all $0 < \varepsilon \leq 1$ in the maximum norm.

3 Consistency

With the solution $a(t, x)$ of the hyperbolic initial value problem (2.4), it is known from [6] that

$$v(t, x) = a(t, x) e^{i(\kappa x - \kappa^2 t/2)/\varepsilon} \quad (3.1)$$

approximates the solution of the nonlinear Schrödinger initial value problem (1.1) up to an $O(\varepsilon)$ error in the maximum norm on a fixed time interval $0 \leq t \leq T$ where a is sufficiently differentiable.

We consider the defect obtained on inserting $v(t, x)$ into the filtered leapfrog scheme (2.1),

$$\begin{aligned} d(t, x) := & i\varepsilon \frac{v(t + \tau, x) - v(t - \tau, x)}{2\tau \operatorname{sinc}(\alpha)} \\ & + \frac{\varepsilon^2}{2} \frac{v(t, x + h) - 2\phi(\beta)v(t, x) + v(t, x - h)}{h^2 \psi(\beta)} - \lambda\varepsilon \frac{|v(t, x)|^2 v(t, x)}{\operatorname{tanc}(\alpha)}. \end{aligned} \quad (3.2)$$

3.1 Defect bound in the maximum norm

Lemma 3.1 *In the situation of Theorem 2.1, the defect (3.2) is bounded in the maximum norm by*

$$\|d\|_{C([0, T] \times \mathbb{T})} \leq c(\tau^2 + h^2 + \varepsilon),$$

where c is independent of ε , τ , h and n with $t_n = n\tau \leq T$.

Proof Using characteristics in (2.4) leads to the ordinary differential equation $i\dot{y} = \lambda|y|^2 y$ whose solutions preserve the norm of the initial value and therefore have bounded derivatives and depend smoothly on the initial value. Since we assumed $a_0 \in C^4(\mathbb{T})$, this argument yields $a \in C^4([0, T] \times \mathbb{T})$. We note

$$\begin{aligned} & v(t + \tau, x) - v(t - \tau, x) \\ &= 2 \left(-i \sin(\alpha) a + \tau \cos(\alpha) \partial_t a - \frac{i\tau^2}{2} \sin(\alpha) \partial_t^2 a + O(\tau^3) \right) e^{i(\kappa x - \kappa^2 t/2)/\varepsilon}, \end{aligned} \quad (3.3)$$

where a and its partial derivatives are evaluated at (t, x) , and similarly

$$\begin{aligned} & v(t, x + h) + v(t, x - h) \\ &= 2 \left(\cos(\beta) a + ih \sin(\beta) \partial_x a + \frac{h^2}{2} \cos(\beta) \partial_x^2 a + O(h^3) \right) e^{i(\kappa x - \kappa^2 t/2)/\varepsilon}. \end{aligned} \quad (3.4)$$

We thus have

$$\begin{aligned} i\varepsilon \frac{v(t + \tau, x) - v(t - \tau, x)}{2\tau \operatorname{sinc}(\alpha)} &= \frac{\kappa^2}{2} \frac{v(t + \tau, x) - v(t - \tau, x)}{-2i \sin(\alpha)} \\ &= \left(\frac{\kappa^2}{2} (a + O(\tau^2)) + \frac{i\varepsilon}{\operatorname{tanc}(\alpha)} (\partial_t a + O(\tau^2)) \right) e^{i(\kappa x - \kappa^2 t/2)/\varepsilon}, \end{aligned}$$

and for ϕ and ψ defined after (2.1) and satisfying (2.5),

$$\begin{aligned} & \frac{\varepsilon^2}{2} \frac{v(t, x + h) - 2\phi(\beta)v(t, x) + v(t, x - h)}{h^2 \psi(\beta)} \\ &= \frac{\kappa^2}{4} \frac{v(t, x + h) - 2\phi(\beta)v(t, x) + v(t, x - h)}{\phi(\beta) - \cos(\beta)} \\ &= \left(\frac{\kappa^2}{2} (-a + O(h^2 + \varepsilon)) + i\varepsilon \frac{\operatorname{sinc}(\beta)}{\psi(\beta)} (\kappa \partial_x a + O(h^2)) \right) e^{i(\kappa x - \kappa^2 t/2)/\varepsilon}. \end{aligned}$$

Here, the $O(h^2 + \varepsilon)$ term requires an explanation: The factor multiplying $\partial_x^2 a$ equals

$$\begin{aligned} & \frac{\varepsilon^2}{2} \frac{1}{h^2 \psi(\beta)} h^2 \cos(\beta) = \frac{1}{2} \varepsilon^2 \frac{\cos(\beta)}{\psi(\beta)} \\ &= \frac{1}{2} \varepsilon^2 \frac{\cos(\beta) - \operatorname{sinc}(\beta)}{\psi(\beta)} + \frac{1}{2} \varepsilon^2 \frac{\operatorname{sinc}(\beta)}{\psi(\beta)} \\ &= -\frac{1}{6} \kappa^2 h^2 + \frac{1}{2} \varepsilon \rho, \end{aligned}$$

where we used the second equation of (2.5) in the last equality. This argument yields the $O(h^2 + \varepsilon)$ term above.

More importantly, the first equation of condition (2.5) ensures that with the solution a of the hyperbolic differential equation (2.4) chosen in (3.1), the defect of v inserted into the numerical scheme becomes small:

$$d(t, x) = \frac{i\varepsilon}{\operatorname{tanc}(\alpha)} \underbrace{\left(\partial_t a + \kappa \partial_x a + i\lambda |a|^2 a \right)}_{=0} + O(\tau^2 + h^2 + \varepsilon).$$

This yields the stated result. \square

However, the maximum norm in the defect bound of Lemma 3.1 turns out to be too weak a norm for the proof of Theorems 2.1 and 2.2.

3.2 Defect bound in the Wiener algebra norm

Let $A(\mathbb{T})$ be the space of 2π -periodic complex-valued functions with absolutely convergent Fourier series $f(x) = \sum_{k=-\infty}^{\infty} \hat{f}(k) e^{ikx}$, equipped with the $\ell^1(\mathbb{Z})$ norm of the sequence of Fourier coefficients. For the pointwise product of two functions $f, g \in A(\mathbb{T})$ we then have (see, e.g., [18, Section I.6])

$$\|fg\|_{A(\mathbb{T})} \leq \|f\|_{A(\mathbb{T})} \|g\|_{A(\mathbb{T})}, \quad (3.5)$$

which makes $A(\mathbb{T})$ a Banach algebra, known as the Wiener algebra. Note that the maximum norm of a function in $A(\mathbb{T})$ is bounded by its $A(\mathbb{T})$ -norm, and conversely, the $A(\mathbb{T})$ -norm is bounded by the maximum norm of the function and its derivative, see [18, Section I.6]:

$$\|f\|_{C(\mathbb{T})} \leq \|f\|_{A(\mathbb{T})} \quad \text{and} \quad \|f\|_{A(\mathbb{T})} \leq c_1 \|f\|_{C^1(\mathbb{T})}. \quad (3.6)$$

The space $C([0, T], A(\mathbb{T}))$ is the Banach space of $A(\mathbb{T})$ -valued continuous functions on the interval $[0, T]$, with $\|d\|_{C([0, T], A(\mathbb{T}))} = \max_{0 \leq t \leq T} \|d(t, \cdot)\|_{A(\mathbb{T})}$.

Lemma 3.2 *In the situation of Theorem 2.1, the defect (3.2) is bounded in the Wiener algebra norm by*

$$\|d\|_{C([0, T], A(\mathbb{T}))} \leq c(\tau^2 + h^2 + \varepsilon),$$

where c is independent of ε , τ , h , and n with $t_n = n\tau \leq T$.

Proof The proof uses the proof of Lemma 3.1 together with the second bound of (3.6), as well as the fact that the absolute sum of the Fourier coefficients of a function is invariant under multiplication of the function with 2π -periodic exponentials e^{ikx} .

The $O(h^3)$ remainder term in (3.4) equals, up to the irrelevant factor $e^{i(\kappa x - \kappa^2 t/2)/\varepsilon}$,

$$s(t, x) = r(t, x, h) e^{i\beta} + r(t, x, -h) e^{-i\beta} \quad \text{with}$$

$$r(t, x, h) = h^3 \int_0^1 \frac{1}{2} (1 - \theta)^2 \partial_x^3 a(t, x + \theta h) d\theta,$$

which for $a \in C([0, T], C^4(\mathbb{T}))$ is bounded by $O(h^3)$ in $C([0, T], C^1(\mathbb{T}))$. The $O(\tau^3)$ remainder term in (3.3) is bounded similarly in $C([0, T], C^1(\mathbb{T}))$, as are all other terms in the proof of Lemma 3.2. So the defect is still bounded by $O(\tau^2 + h^2 + \varepsilon)$ in the $C([0, T], C^1(\mathbb{T}))$ norm, and thus by (3.6) also in the $C([0, T], A(\mathbb{T}))$ norm. \square

While we have only considered the filtered leapfrog method so far, an analogous proof shows that the defect of the filtered Crank–Nicolson method satisfies the same bound as in Lemma 3.2.

4 Stability

4.1 Linear stability analysis in the Wiener algebra

In this subsection we give linear stability results for the filtered leapfrog and Crank–Nicolson schemes. We bound numerical solutions corresponding to the linear Schrödinger equation (1.1) (without the nonlinearity) in the Wiener algebra norm, using Fourier analysis.

We momentarily omit the nonlinearity and interpolate the filtered leapfrog scheme (2.1) from discrete spatial points $x_j = jh$ to arbitrary $x \in \mathbb{T}$ by setting

$$i\varepsilon \frac{u^{n+1}(x) - u^{n-1}(x)}{2\tau \operatorname{sinc}(\alpha)} + \frac{\varepsilon^2}{2} \frac{u^n(x+h) - 2\phi(\beta)u^n(x) + u^n(x-h)}{h^2 \psi(\beta)} = 0. \quad (4.1)$$

We clearly have $u^n(x_j) = u_j^n$ of (2.1) for all $n \geq 2$ if this holds true for $n = 0$ and $n = 1$. In particular, we have $\max_j |u_j^n| \leq \max_{x \in \mathbb{T}} |u^n(x)| \leq \|u^n\|_{A(\mathbb{T})}$.

Lemma 4.1 (Linear stability of the filtered leapfrog method) *Under condition (2.6), the filtered leapfrog algorithm (4.1) without the nonlinear term is stable: There exists a norm $\|\cdot\|$ on $A(\mathbb{T}) \times A(\mathbb{T})$, equivalent to the norm $\|\cdot\|_{A(\mathbb{T}) \times A(\mathbb{T})}$ uniformly in ε, τ, h subject to (2.6), such that*

$$\|U^n\| = \|U^{n-1}\|, \quad \text{where } U^n = \begin{pmatrix} u^{n+1} \\ u^n \end{pmatrix}.$$

Proof Let $\hat{u}^n = (\hat{u}_k^n)$ be the sequence of Fourier coefficients of u^n , i.e.,

$$u^n(x) = \sum_{k=-\infty}^{\infty} e^{ikx} \hat{u}_k^n.$$

Substituting this into (4.1) yields, for all j ,

$$\sum_k e^{ikx_j} \left(i\varepsilon \frac{\hat{u}_k^{n+1} - \hat{u}_k^{n-1}}{2\tau \operatorname{sinc}(\alpha)} + \varepsilon^2 \frac{\cos(kh) - \phi(\beta)}{\psi(\beta)} \hat{u}_k^n \right) = 0,$$

and thus

$$i\varepsilon \frac{\hat{u}_k^{n+1} - \hat{u}_k^{n-1}}{2\tau \operatorname{sinc}(\alpha)} + \varepsilon^2 \frac{\cos(kh) - \phi(\beta)}{\psi(\beta)} \hat{u}_k^n = 0,$$

which is equivalent to the system

$$\begin{pmatrix} \hat{u}_k^{n+1} \\ \hat{u}_k^n \end{pmatrix} = G_k \begin{pmatrix} \hat{u}_k^n \\ \hat{u}_k^{n-1} \end{pmatrix},$$

where

$$G_k = \begin{pmatrix} 2i\mu_k & 1 \\ 1 & 0 \end{pmatrix} \quad \text{with} \quad \mu_k = \frac{\varepsilon\tau}{h^2} \operatorname{sinc}(\alpha) \frac{\cos(kh) - \phi(\beta)}{\psi(\beta)}. \quad (4.2)$$

Let λ_k^+, λ_k^- be the two roots of the characteristic polynomial

$$\rho_k(\zeta) = \zeta^2 - 2i\mu_k\zeta - 1,$$

i.e.,

$$\lambda_k^\pm = i\mu_k \pm (1 - \mu_k^2)^{1/2}.$$

Under condition (2.6), we have $|\mu_k| < 1$ and thus $|\lambda_k^\pm| = 1$. The vectors $(\lambda_k^+, 1)^\top$ and $(\lambda_k^-, 1)^\top$ are eigenvectors of G_k with eigenvalue λ_k^+ and λ_k^- , respectively. This is because (similar for λ_k^-)

$$\begin{pmatrix} 2i\mu_k & 1 \\ 1 & 0 \end{pmatrix} \begin{pmatrix} \lambda_k^+ \\ 1 \end{pmatrix} = \begin{pmatrix} 2i\mu_k\lambda_k^+ + 1 \\ \lambda_k^+ \end{pmatrix} = \lambda_k^+ \begin{pmatrix} \lambda_k^+ \\ 1 \end{pmatrix}.$$

Therefore G_k is diagonalizable,

$$P_k^{-1}G_kP_k = \Lambda_k = \text{diag}\{\lambda_k^+, \lambda_k^-\}, \quad (4.3)$$

and Λ_k is a unitary matrix. Using the transformation matrix P_k , we have, for any vector $y \in \mathbb{C}^2$,

$$|P_k^{-1}G_ky|_2 = |\Lambda_kP_k^{-1}y|_2 = |P_k^{-1}y|_2.$$

Therefore,

$$\begin{aligned} \|U^n\| &:= \sum_k \left| P_k^{-1} \begin{pmatrix} \hat{u}_k^{n+1} \\ \hat{u}_k^n \end{pmatrix} \right|_2 = \sum_k \left| P_k^{-1}G_k \begin{pmatrix} \hat{u}_k^n \\ \hat{u}_k^{n-1} \end{pmatrix} \right|_2 \\ &= \sum_k \left| P_k^{-1} \begin{pmatrix} \hat{u}_k^n \\ \hat{u}_k^{n-1} \end{pmatrix} \right|_2 = \|U^{n-1}\|. \end{aligned}$$

Finally, we show that

$$\|P\|_2 := \max_k \|P_k\|_2 \leq C_1, \quad \|P^{-1}\|_2 := \max_k \|P_k^{-1}\|_2 \leq C_2,$$

which yields that the newly introduced norm $\|\cdot\|$ is equivalent to $\|\cdot\|_{A(\mathbb{T}) \times A(\mathbb{T})}$. Since

$$P_k^*P_k = \begin{pmatrix} \frac{2}{1 + \overline{\lambda_k^-}\lambda_k^+} & 1 + \overline{\lambda_k^+}\lambda_k^- \\ 1 + \overline{\lambda_k^-}\lambda_k^+ & 2 \end{pmatrix},$$

the eigenvalues of $P_k^*P_k$ can be calculated as $2(1 \pm \mu_k)$. Since $|\mu_k| \leq \theta < 1$ by condition (2.6), we have for all k that

$$\begin{aligned} \|P_k\|_2 &= \sqrt{\lambda_{\max}(P_k^*P_k)} < 2, \\ \|P_k^{-1}\|_2 &= 1/\sqrt{\lambda_{\min}(P_k^*P_k)} \leq 1/\sqrt{2(1-\theta)}, \end{aligned}$$

so that

$$\frac{1}{2} \|U\|_{A(\mathbb{T}) \times A(\mathbb{T})} \leq \|U\| \leq \frac{1}{\sqrt{2(1-\theta)}} \|U\|_{A(\mathbb{T}) \times A(\mathbb{T})}$$

for all $U \in A(\mathbb{T}) \times A(\mathbb{T})$. \square

We similarly extend the filtered Crank–Nicolson algorithm (2.2) to all $x \in \mathbb{T}$ and omit the nonlinearity.

Lemma 4.2 (Linear stability of the filtered Crank–Nicolson method) *The filtered Crank–Nicolson algorithm (2.2) without the nonlinear term is unconditionally stable with*

$$\|u^{n+1}\|_{A(\mathbb{T})} = \|u^{n-1}\|_{A(\mathbb{T})}.$$

Proof Substituting the Fourier series of u^n into (2.2) without the nonlinear term yields

$$\sum_k e^{ikx} \left(i\varepsilon \frac{\hat{u}_k^{n+1} - \hat{u}_k^{n-1}}{2\tau \operatorname{sinc}(\alpha)} + \varepsilon^2 \frac{\cos(kh) - \phi(\beta)}{h^2 \psi(\beta)} \frac{\hat{u}_k^{n+1} + \hat{u}_k^{n-1}}{2 \cos(\alpha)} \right) = 0,$$

which leads to

$$\begin{aligned} & \left(\frac{i\varepsilon}{2\tau \operatorname{sinc}(\alpha)} + \frac{\varepsilon^2}{2 \cos(\alpha)} \frac{\cos(kh) - \phi(\beta)}{h^2 \psi(\beta)} \right) \hat{u}_k^{n+1} \\ &= \left(\frac{i\varepsilon}{2\tau \operatorname{sinc}(\alpha)} - \frac{\varepsilon^2}{2 \cos(\alpha)} \frac{\cos(kh) - \phi(\beta)}{h^2 \psi(\beta)} \right) \hat{u}_k^{n-1}. \end{aligned}$$

Therefore we have $|\hat{u}_k^{n+1}| = |\hat{u}_k^{n-1}|$ for all k , which yields the result. \square

4.2 Nonlinear stability

Lemma 4.3 (Nonlinear stability of the filtered leapfrog method) *Let the function $v \in C([0, T], A(\mathbb{T}))$ be arbitrary and let the corresponding defect d be defined by (3.2). Under condition (2.6), the interpolated numerical solution of (2.1), interpolated to all $x \in \mathbb{T}$ as in (4.1) (but now with the nonlinear term included), satisfies the bound, for $t_n = n\tau \leq T$*

$$\|u^n - v(t_n, \cdot)\|_{A(\mathbb{T})} \leq C \left(\|u^0 - v(0, \cdot)\|_{A(\mathbb{T})} + \|u^1 - v(t_1, \cdot)\|_{A(\mathbb{T})} + \|d\|_{C([0, T], A(\mathbb{T}))} \right),$$

where C is independent of ε , τ , h , and n with $t_n \leq T$, but depends on T and on upper bounds of the above term in big brackets and of the $C([0, T], A(\mathbb{T}))$ norm of v .

Proof We define the error function $e^n(x) = u^n(x) - v(t_n, x)$, which satisfies

$$\begin{aligned} e^{n+1}(x) - e^{n-1}(x) &= \frac{i\varepsilon^2 \tau \operatorname{sinc}(\alpha)}{h^2 \psi(\beta)} (e^n(x+h) - 2\phi(\beta)e^n(x) + e^n(x-h)) \\ &\quad - 2i\lambda\tau \cos(\alpha) (|u^n(x)|^2 u^n(x) - |v^n(x)|^2 v^n(x)) - \frac{2i\tau \operatorname{sinc}(\alpha)}{\varepsilon} d(t_n, x). \end{aligned} \tag{4.4}$$

The discrete Fourier transform of e^n then satisfies

$$\begin{aligned} \hat{e}_k^{n+1} - \hat{e}_k^{n-1} &= \frac{i\varepsilon^2 \tau \operatorname{sinc}(\alpha) (\cos(kh) - \phi(\beta))}{h^2 \psi(\beta)} \hat{e}_k^n \\ &\quad - 2i\tau \cos(\alpha) \lambda \mathcal{F}(|u^n|^2 u^n - |v^n|^2 v^n)(k) - 2i\tau \cos(\alpha) \rho^{-1} \hat{d}_k^n, \end{aligned}$$

where we used (2.5) in the last term. This equation is equivalent to the one-step formulation

$$\begin{pmatrix} \hat{e}_k^{n+1} \\ \hat{e}_k^n \end{pmatrix} = G_k \begin{pmatrix} \hat{e}_k^n \\ \hat{e}_k^{n-1} \end{pmatrix} - 2i\tau \cos(\alpha) \lambda \begin{pmatrix} \mathcal{F}(|u^n|^2 u^n - |v^n|^2 v^n)(k) \\ 0 \end{pmatrix} \\ - 2i\tau \cos(\alpha) \rho^{-1} \begin{pmatrix} \hat{d}_k^n \\ 0 \end{pmatrix},$$

where G_k is defined in (4.2).

Introducing $\mathcal{E}^n = \begin{pmatrix} e^{n+1} \\ e^n \end{pmatrix}$, using Lemma 4.1 and (3.5) for dealing with the nonlinearity, we obtain

$$\begin{aligned} \|\mathcal{E}^n\| &\leq (1 + c\tau) \|\mathcal{E}^{n-1}\| + \tilde{c}\tau \|d(t_n, \cdot)\|_{A(\mathbb{T})} \\ &\leq (1 + c\tau)^n \|\mathcal{E}^0\| + \tilde{c}\tau \sum_{j=1}^n (1 + c\tau)^{n-j} \|d(t_j, \cdot)\|_{A(\mathbb{T})} \\ &\leq \exp(cn\tau) \|\mathcal{E}^0\| + \tilde{c}\tau \frac{\exp(cn\tau) - 1}{c\tau} \sup_{t \in [0, T]} \|d(t, \cdot)\|_{A(\mathbb{T})}, \end{aligned}$$

which yields the result. \square

An analogous result holds true for the filtered Crank–Nicolson method, with essentially the same proof, now based on Lemma 4.2.

Combined with Lemma 3.2 (consistency), Lemma 4.3 (stability) proves Theorem 2.1 with the $O(\tau^2 + h^2 + \varepsilon)$ remainder bound in the Wiener algebra norm, which is stronger than the maximum norm and hence this yields the same bound in the maximum norm. Theorem 2.1 together with [6, Theorem 6.5] further implies the error bound of Theorem 2.2.

5 Numerical experiments

In this section, we consider the one dimensional semiclassical nonlinear Schrödinger equation

$$i\varepsilon \partial_t u + \frac{\varepsilon^2}{2} \partial_{xx} u = \varepsilon |u|^2 u$$

with the initial value

$$u(0, x) = e^{-x^2} e^{ix/\varepsilon},$$

and we choose $x \in [-4, 4]$ with periodic boundary conditions.

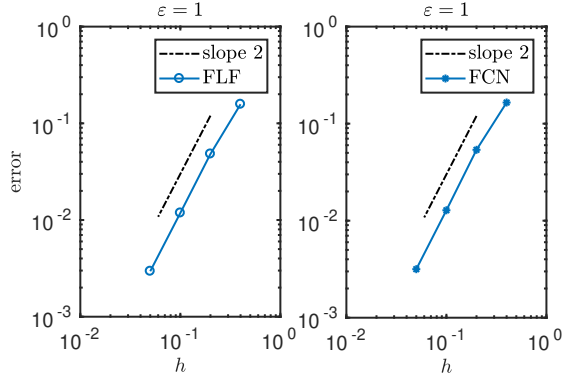


Fig. 5.1 Error vs. h with $\varepsilon = 1$ for filtered leapfrog method (left column) and filtered Crank–Nicolson method (right column).

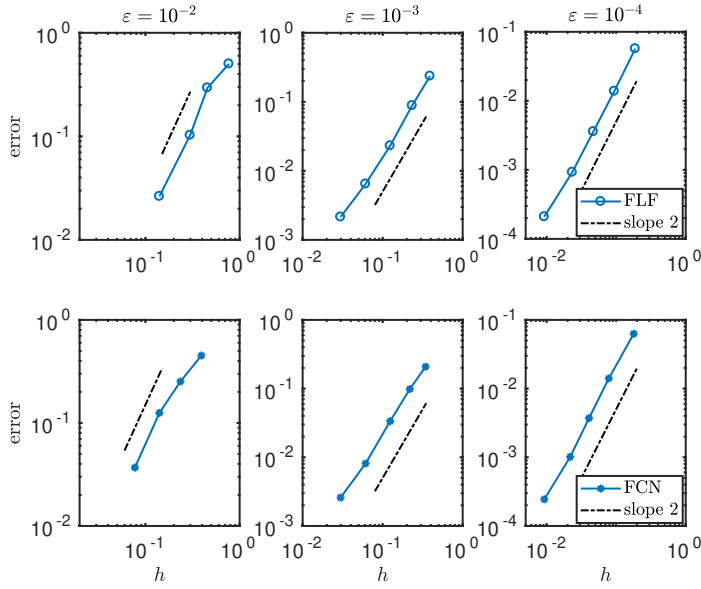


Fig. 5.2 Error vs. h with small ε for filtered leapfrog method (top row) and filtered Crank–Nicolson method (bottom row).

We first test our algorithms with $\varepsilon = 1$. In this case the solution of (1.1) is not highly oscillatory, and condition (2.5) is not required in our implementation. We select different mesh sizes $h = 0.4, 0.2, 0.1, 0.05$ and accordingly, the time step is set as $\tau = h^2/4$ for the filtered leapfrog method and $\tau = h/8$ for the filtered Crank–Nicolson method. The reference solution is obtained using Fourier collocation with 6000 grid points in space and Strang splitting with time step 10^{-4} in time.

Since the filtered leapfrog and filtered Crank–Nicolson methods converge to the standard leapfrog and standard Crank–Nicolson methods, respectively, we observe second-order accuracy in Figure 5.1. The errors for both methods are measured at the final time $T = 1$ using the discrete L^∞ norm over $[-4, 4]$.

For small ε , condition (2.5) is necessary. We first set ρ and then obtain α by solving the nonlinear equation $\frac{\varepsilon}{\tan(\alpha)} = \rho$, which can be accomplished using the “fsolve” function in MATLAB. It is noted that starting with $\alpha = n\pi, n \neq 0$ is generally a good choice. The time step can be determined immediately after obtaining α . Similarly, we can find β by solving the relation $\frac{\varepsilon \operatorname{sinc}(\beta)}{\psi(\beta)} = \rho$ with the starting value $\beta = \kappa\tau/(m\varepsilon), m \neq 0$, where m is introduced to satisfy the stability condition (2.6). In this example, we choose $\rho = 4$.

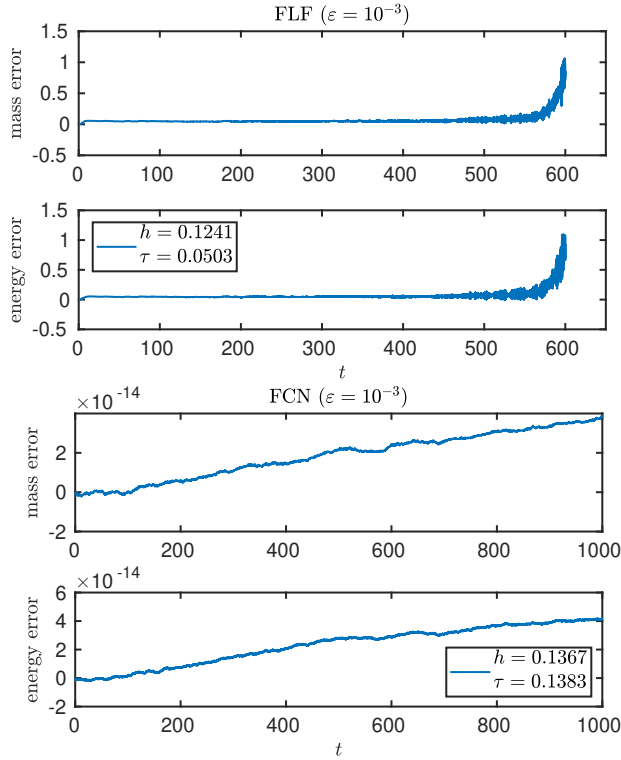


Fig. 5.3 Relative error of discrete mass and energy (2.3) as a function of time, along the numerical solution of the filtered leapfrog method (top) and filtered Crank–Nicolson method (bottom).

Figure 5.2 illustrates the accuracy order of the two methods for small ε , which is consistent with our theoretical estimate presented in Theorem 2.2. Both methods demonstrate second-order accuracy for small ε with relatively large mesh sizes. The error is again measured at the final time $T = 1$ using the discrete counterpart of the maximum norm on $[-4, 4]$.

We also investigate the long-time behavior of the filtered Crank–Nicolson method. Figure 5.3 shows the evolution of the relative error of discrete mass and energy (2.3) for $\varepsilon = 10^{-3}$ over a long-time interval. It is observed that the filtered Crank–Nicolson scheme (2.2) preserves the discrete mass and energy very well, even with large time step and mesh size. In this test, we set the iteration tolerance as 10^{-14} . The filtered leapfrog method approximately preserves the discrete mass and energy well over a rather long time interval $t \leq 400$ but then the numerical solution blows up. The interval gets longer when the time step τ is reduced.

Acknowledgement

This work was supported by the Deutsche Forschungsgemeinschaft (DFG, German Research Foundation) – Project-ID258734477 – SFB 1173.

References

1. A. Arnold, N. B. Abdallah, and C. Negulescu. WKB-based schemes for the oscillatory 1D Schrödinger equation in the semiclassical limit. *SIAM Journal on Numerical Analysis*, 49(4):1436–1460, 2011.
2. W. Bao, S. Jin, and P. A. Markowich. On time-splitting spectral approximations for the Schrödinger equation in the semiclassical regime. *Journal of Computational Physics*, 175(2):487–524, 2002.
3. W. Bao, S. Jin, and P. A. Markowich. Numerical study of time-splitting spectral discretizations of nonlinear Schrödinger equations in the semiclassical regimes. *SIAM Journal on Scientific Computing*, 25(1):27–64, 2003.
4. C. Besse, R. Carles, and F. Méhats. An asymptotic preserving scheme based on a new formulation for NLS in the semiclassical limit. *Multiscale Modeling & Simulation*, 11(4):1228–1260, 2013.
5. R. Carles. *Semi-classical analysis for nonlinear Schrödinger equations—WKB analysis, focal points, coherent states*. World Scientific Publishing Co., Singapore, second edition, 2021.
6. R. Carles, E. Dumas, and C. Sparber. Multiphase weakly nonlinear geometric optics for Schrödinger equations. *SIAM Journal on Mathematical Analysis*, 42(1):489–518, 2010.
7. P. Degond, S. Gallego, and F. Méhats. An asymptotic preserving scheme for the Schrödinger equation in the semiclassical limit. *Comptes Rendus Mathématique*, 345(9):531–536, 2007.
8. M. Delfour, M. Fortin, and G. Payr. Finite-difference solutions of a non-linear Schrödinger equation. *Journal of Computational Physics*, 44(2):277–288, 1981.
9. B. Garcia-Archilla, J. M. Sanz-Serna, and R. D. Skeel. Long-time-step methods for oscillatory differential equations. *SIAM Journal on Scientific Computing*, 20(3):930–963, 1998.
10. E. Grenier. Semiclassical limit of the nonlinear Schrödinger equation in small time. *Proceedings of the American Mathematical Society*, 126(2):523–530, 1998.
11. V. Grimm and M. Hochbruck. Error analysis of exponential integrators for oscillatory second-order differential equations. *Journal of Physics A: Mathematical and General*, 39(19):5495, 2006.
12. E. Hairer and C. Lubich. Long-time energy conservation of numerical methods for oscillatory differential equations. *SIAM Journal on Numerical Analysis*, 38(2):414–441, 2000.
13. E. Hairer, C. Lubich, and Y. Shi. Large-stepsizes integrators for charged-particle dynamics over multiple time scales. *Numerische Mathematik*, 151(3):659–691, 2022.

14. E. Hairer, C. Lubich, and B. Wang. A filtered Boris algorithm for charged-particle dynamics in a strong magnetic field. *Numerische Mathematik*, 144:787–809, 2020.
15. E. Hairer, C. Lubich, and G. Wanner. *Geometric numerical integration. Structure-preserving algorithms for ordinary differential equations*. Springer Series in Computational Mathematics 31. Springer-Verlag, Berlin, 2002.
16. M. Hochbruck and C. Lubich. A Gautschi-type method for oscillatory second-order differential equations. *Numerische Mathematik*, 83:403–426, 1999.
17. S. Jin, P. Markowich, and C. Sparber. Mathematical and computational methods for semiclassical Schrödinger equations. *Acta Numerica*, 20:121–209, 2011.
18. Y. Katznelson. *An introduction to harmonic analysis*. Dover Publications, Inc., New York, corrected edition, 1976.
19. C. Lasser and C. Lubich. Computing quantum dynamics in the semiclassical regime. *Acta Numerica*, 29:229–401, 2020.
20. E. Madelung. Quantum theory in hydrodynamical form. *Zeitschrift für Physik*, 40:322, 1927.
21. P. A. Markowich, P. Pietra, and C. Pohl. Numerical approximation of quadratic observables of Schrödinger-type equations in the semi-classical limit. *Numerische Mathematik*, 81:595–630, 1999.